



Mechanism of lysozyme adsorption onto gold surface determined by quartz crystal microbalance and surface plasmon resonance

P. Komorek, M. Wałek, B. Jachimska *

Jerzy Haber Institute of Catalysis and Surface Chemistry Polish Academy of Sciences, Niezapominajek 8, 30-239 Cracow, Poland

ARTICLE INFO

Article history:

Received 2 March 2020

Received in revised form 2 June 2020

Accepted 2 June 2020

Available online 6 June 2020

Keywords:

Lysozyme adsorption

Gold surface

Quartz crystal microbalance with dissipation

Surface plasmon resonance

ABSTRACT

In this study, the physicochemical characterization of lysozyme adsorbed on gold was investigated. Through the use of MP-SPR it was possible to establish that the orientation of molecules changes from *side-on* to *between* or *end-on* with increasing surface coverage. The data confirms that the process of adsorption is driven primarily by electrostatic interactions but also by hydrophobic forces. MP-SPR data was compared with the Random Sequential Adsorption model for a molecule with an ellipsoidal shape. Contact angle measurements showed that higher surface coverage also translates in more hydrophilic properties of obtained lysozyme layer. Comparison of CD and PM-IRRAS spectra in solution and adsorbed state respectively showed changes in the secondary structures of lysozyme. These changes are dependent on pH, but fundamentally they go in the direction of the increase of β -turn/random content with a simultaneous decrease in β -sheet fraction, which suggests that aggregation is not occurring. The combination of MP-SPR and QCM-D measurements allowed the estimation of the number of water molecules associated with the lysozymes films. It has been observed that hydration decreases from 70% in pH = 4 to 30% in pH = 11. This data indicates that hydration is driven mainly by the degree of protonation of lysozyme molecules.

© 2020 Elsevier B.V. All rights reserved.

1. Introduction

The implementation of proteins in biomedical applications has recently gained more and more attention. Progressively proteins are tested as substrates for modification of implantable devices [1–4], producing agents supporting tissue regeneration [5–7], or designing drug delivery systems [8–12]. As materials used in the field of medicine must be characterized by biocompatibility, controlled biodegradability, non-immunogenicity, structural integrity, and non-toxicity, the characteristics of the physicochemical properties of proteins (which have a direct impact on the listed attributes) are particularly important. Adsorption is one of the processes that can significantly affect the physicochemical properties of biomolecules used in biomedical systems [13–15].

Although the adsorption process has already been extensively studied and many ambiguities have already been clarified, the mechanism of protein adsorption and its effects are still not fully understood. The effects of the adsorption process are dependent on, amongst others, the amount of immobilized protein, which can be determined using methods providing real-time measure-

ments like quartz crystal microbalance [16,17], surface plasmon resonance [18–20] or ellipsometry [21,22]. K. Xu et al. showed that the amount of adsorbed protein and, therefore surface coverage affects the reversibility of adsorption and orientation of adsorbed molecules [23]. Other studies confirmed that adsorption under various conditions is associated with changes in the secondary structure of molecules, which is significant as changes in conformation can be related to the induction of biomolecules' toxicity [24].

Not only microscopic but also macroscopic properties can be associated with the process of adsorption. For example, wettability properties depend on protein protonation [25,26], and pH influences the hydrophobic properties of protein films [27]. Properties of adsorbed molecules can also be modified by solvent coupled within the protein layer, but only a few studies examined its role [28].

In the presented work, we selected hen egg lysozyme and gold surface to study factors that have a significant impact on the mechanism of protein adsorption and to determine the hydration of the protein layer on the solid surface. Lysozyme is resistant to substantial changes in its structure. However, it is considered as amyloidogenic protein and precursor of some amyloidosis [29]. There are several factors that affect the conformational changes of amyloidogenic proteins and consequently lead to the formation of aggregates or amyloid fibrils. These factors include temperature, pH,

* Corresponding author.

E-mail address: ncjachim@cyf-kr.edu.pl (B. Jachimska).

high ionic strength, or surface type - mainly characterized by hydrophobic properties [30–33]. Therefore, we decided to study the mechanism of adsorption of lysozyme on the gold surface under various pH conditions in order to identify changes in the secondary structure of lysozyme towards aggregation or amyloid formation under selected conditions.

By using surface plasmon resonance (MP-SPR) and quartz crystal microbalance (QCM-D) the nature of the interactions and related amount of adsorbed protein were investigated and allowed us to determine an orientation of molecules on the surface. Experimental data were compared with a Random Sequential Adsorption model for ellipsoidal shape molecules.

Further comparison of the secondary structure of lysozyme in the solution obtained by circular dichroism and in adsorbed state measured by Fourier transform spectroscopy gave insight into the stability of lysozyme conformation and suggested, that the changes in lysozyme secondary structure do not go in the direction of aggregation. These detailed characteristics of factors determining protein adsorption and effects resulting from this process will contribute to a better understanding of the control of biomolecule adsorption for biomedical and biotechnology applications.

2. Materials and methods

2.1. Materials

The study used lysozyme from egg white. Lysozyme (L6876) was purchased from Sigma-Aldrich and used without further purification. Lysozyme solutions were prepared for all measurements by dissolving protein powder in aqueous solutions with 0.01 M NaCl ionic strength. The pH of the solutions was controlled in the range of 3.0–11.0 by adding small amounts of HCl or NaOH. The pH of lysozyme and NaCl solutions was monitored using a precision WTW pH meter equipped with a Hamilton Polyplast Din electrode. All experiments were performed at 298 K. Preparation solutions immediately prior to measurement. Lysozyme adsorption was carried out on MP-SPR and QCM sensors covered with a layer of gold. The sensors were cleaned before each measurement. All chemicals used were purchased from Sigma-Aldrich.

2.2. Methods

2.2.1. Circular dichroism (CD)

The structure of lysozyme in a 0.01 M solution of NaCl at varied pH (in the range 3.0–10.0) was monitored using a Circular Dichroism (CD) using a Jasco-1500 spectrometer with a 10 nm quartz cuvette. Solvent base spectra were measured using 0.01 M NaCl under defined pH conditions. The concentration of lysozyme solutions in 0.01 M NaCl was 50 ppm. The spectra were recorded in the wavelength range 185–300 nm with a resolution of 1 nm and a scanning speed of 50 nm/min. Qualitative and quantitative analysis of the secondary structure of lysozyme under various pH conditions was carried out using Jasco software.

2.2.2. Measurements of electrophoretic mobility

Measurements of electrophoretic mobility of lysozyme were carried out using Zeta Malvern Zetasizer Nano ZS. The concentration of the lysozyme solution was 1000 ppm with a controlled ionic strength of $I = 0.01$ M in the pH range of 3–10.5. The zeta potential of lysozyme molecules was calculated using the Henry equation.

2.2.3. Multi-parameter surface plasmon resonance (MP-SPR)

The kinetics of lysozyme adsorption on the surface of gold was monitored by surface plasmon resonance (BioNavis SPR Navi™ 200) while varying the pH in the range of 4.0–9.0. The instrument is

equipped with an angle scanning goniometer with two independent fluid channels, a prismatic clutch (Krechmer mode) and an integrated peristaltic pump to control flow conditions. The MP-SPR angular range is 40–78° at 670 and 785 nm. MP-SPR measurements were carried out by determining the baseline for the NaCl solution at a specified ionic strength (0.01 M NaCl) and pH (10 min), then 90 min of lysozyme adsorption (5 ppm, 0.01 M NaCl) at the appropriate pH and 90 min of rinsing 0.01 M NaCl (suitable pH). Adsorption of protein on the sensor surface can be monitored by changing the intensity at a fixed angle or in an angular position over time. The thickness and refractive index of adsorbed films were determined using the Navi™ LayerSolver software for a wavelength of 670 nm.

2.2.4. Quartz microbalance with energy dissipation monitoring (QCM-D)

The efficiency of lysozyme adsorption on the gold surface and the properties of the formed layer was also determined at different pH of lysozyme using a quartz microbalance with energy dissipation monitoring (QSense E1, Biolin Scientific) with a flow module. The scattering monitoring module provides a description of the viscoelastic properties of the layer formed on the sensor. Sensors covered with a layer of gold characterized by a resonant frequency equal to $4.95 \text{ MHz} \pm 50 \text{ Hz}$ were used for all measurements. Flow rates were controlled by a peristaltic pump (Ismatec). The measurement series were carried out in the same mode as the MP-SR experiments: solvent baseline (10 min NaCl), 90 min adsorption of lysozyme, followed by washing with a solution of NaCl for 90 min. The adsorbed mass on the sensor for homogeneous, rigid films was calculated using the Sauerbrey model. The layer thickness for each pH was calculated, assuming the effective density depending on the degree of hydration:

$$\rho_{\text{film}} = \frac{\rho_{\text{LYS}} \cdot V_{\text{LYS}} + \rho_{\text{NaCl}} \cdot V_{\text{NaCl}}}{V_{\text{LYS}} + V_{\text{NaCl}}} \quad (1)$$

where ρ_{NaCl} is the density of the NaCl solution, ρ_{LYS} is the density of lysozyme solution, V_{LYS} is the volume fraction of the lysozyme in solution, and V_{NaCl} is the volume fraction of solvent in the film. The density of the solvent and lysozyme was measured using an Anton Paar DMA 5000 M densitometer ($\rho_{\text{LYS}} = 1.33 \text{ g/cm}^3$) [34].

2.2.5. PM-IRRAS

The secondary structure of lysozyme in the adsorbed state was measured using a vertex 70 spectrometer with polarization modulation set (PMA 50, Bruker, Ettlingen, Germany) with photoelastic modulator (PEM) and demodulator (Hinds Instruments, Hillsboro, USA). A 100 nm gold layer was applied to the glass plate by vapor deposition. Measurements were made in the range of wavelengths from 700 to 4000 cm^{-1} . 400 scans were averaged with 4 cm^{-1} spectral resolution for each spectrum, and the incidence angle was 80°. Lysozyme was adsorbed on the surface at different pH (3.0–11.0) for protein concentration $c = 50$ ppm for $I = 0.01$ M NaCl solution. The adsorption time was 90 min, then the adsorption surface was washed successively with 0.01 M NaCl solution and water for 90 min. Qualitative and quantitative analysis of the structure of secondary lysozyme was carried out using OPUS v5.5 software (Bruker, Ettlingen, Germany).

2.2.6. Contact angle measurements (CA)

Contact angles were measured by determining the shape of the sedentary water drop using axial symmetrical drop shape analysis (ADSA) with a system accuracy of 1°. A layer of lysozyme was deposited on the surface according to the procedure outlined in Section 2.2.5. After lysozyme adsorption, the sensor was dried with a delicate stream of air and then placed in a thermostated chamber. The image of a drop of sitting water was obtained with a CCD video

camera. The Young-Laplace equation was fitted to the digitized water drop profile on the sensor surface.

3. Results and discussion

3.1. Physicochemical properties of lysozyme

The structural stability of lysozyme in aqueous solutions was controlled by the circular dichroism (CD) method in a wide range of UV-Vis wavelengths (185–250 nm). On the recorded CD spectra (Fig. 1) two strong, negative bands at 208 nm and 222 nm are characteristic, also one positive band at 193 nm [35], which corresponds to α -helical structures. Other strong bands characteristic of a well-defined β -sheet occur at 218 nm (negative) and 195 nm (positive) [36]. The obtained spectra show that when the pH of the lysozyme solution changes, there are no major structural changes, which indicates that lysozyme is stable under such experimental conditions and no significant changes in its secondary structure occurred. The average estimated content of α -helix in lysozyme in NaCl solution is 35.7%, β -sheets – 31.1%, β -turn – 1.2%, and random structures occur at 32.0%. The results obtained are consistent with the CD measurements obtained by Chang et al. (α -helix – 30%, β -sheets – 35%, β -turn – 6%, and random structures occur at 30.0%) [37]. For comparison, the results for the secondary structure obtained by X-ray method are α -helix – 41%, β -sheets – 16%, β -turn – 23% and random structures – 20% [37]. The differences in obtained results come from the state in which the sample was tested, which is associated with interactions in the crystalline and liquid states, as well as with the method of analyzing the results.

To estimate the interactions between the protein and the gold surface, the zeta potential of the protein molecules were measured for the ionic strength $I = 0.01$ M NaCl in a wide pH range and compared with a zeta potential of QCM-D gold sensor. The zeta potential of the gold surface was presented in our previous publication (Fig. 2) [38]. In the case of protein, the zeta potential value strongly depends on the pH of the solution. The zeta potential reaches 50.0 mV for pH = 3.0 and drops to –7 mV for pH = 10.5. For gold surface, the potential varies from 7.0 mV for pH = 3.0 to –38.0 mV for pH = 10.5. The determined isoelectric points occur at pH = 10.0 and pH = 3.4, respectively, for the lysozyme molecule and the gold surface. L. R. Wetter and Deutsh established the isoelectric point for lysozyme at pH = 11.35 in glycine buffer with an ionic strength of 0.1 M [39], whereas C.A. Haynes and W. Norde at pH = 11.1 [40]. The differences in isoelectric point are associated

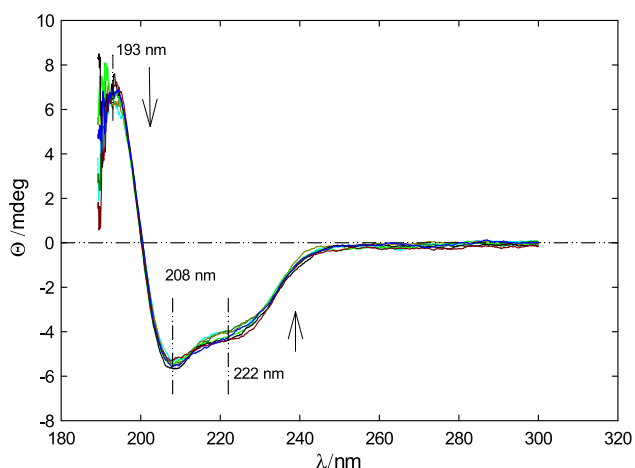


Fig. 1. CD spectra of lysozyme in solutions at ionic strength $I = 0.01$ M NaCl. Each curve corresponds to a different pH in the range of 3.0–11.0.

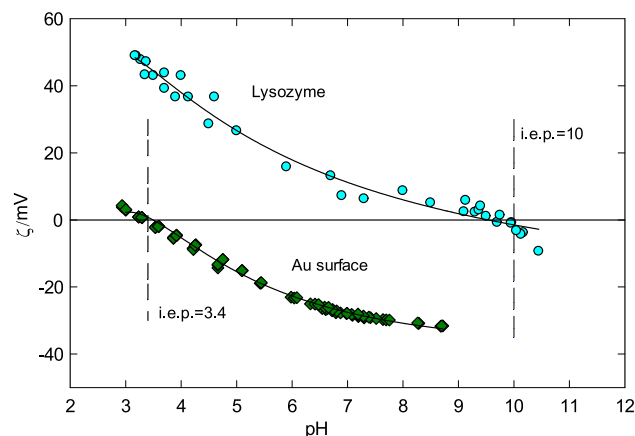


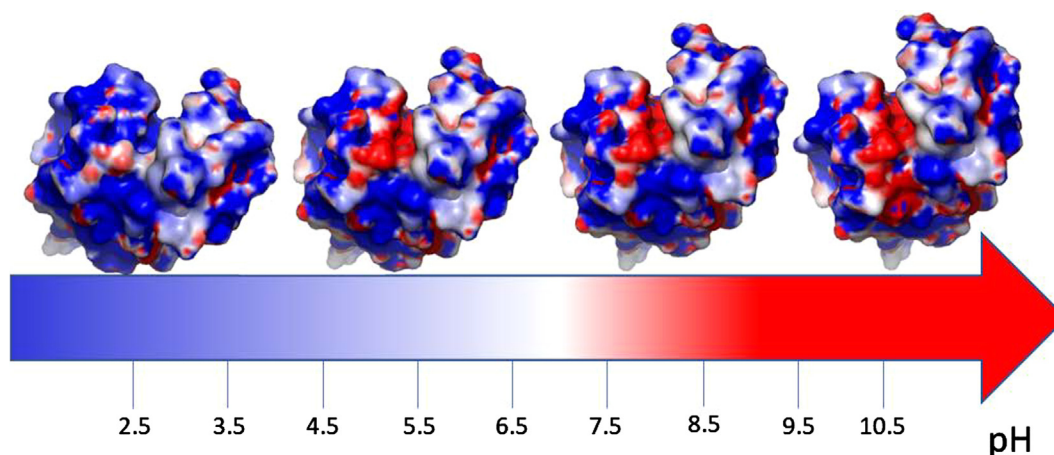
Fig. 2. Zeta potential of lysozyme and the surface of QCM-D gold surface as a function of pH at 0.01 M NaCl ionic strength. The results for lysozyme are marked in cyan and for the sensor dark green, i.e.p. - indicates isoelectric point [38].

with specific and non-specific adsorption of ions on the protein surface in various buffers. The conducted research allows us to conclude that in the pH range between 3.4 and 10.0, there are attractive electrostatic interactions between positively charged lysozyme particles and a negatively charged surface. By adsorption, the positively charged particles neutralize the negatively charged surface.

It should be noted that in the case of proteins, the charge distribution on their surface is very asymmetrical. In Schematic 1 distribution of positively and negatively charged domains (positive - blue, negative - red, neutral - white) on the surface of lysozyme depending on the pH for 0.01 M NaCl is shown. Visualization was prepared using the 1iee structure from the RCS protein database in the PyMOL software package. The obtained distribution indicates that in the case of lysozyme, the surface charge is not regularly distributed on the surface of the protein. From the literature, it is known that the most positively charged areas are N, C-terminal surface and its opposite side, in the middle, there are both positive and negative charged areas [41]. It can be expected that during the adsorption process, a negatively charged gold surface will prefer contact with positively charged residues by electrostatic attraction, which drives the adsorption process and forces the molecule to specific orientate relative to the surface. It is worth considering that hydrophobic interactions can also play an important role in the adsorption process. The positively charged regions correspond to the hydrophilic areas, so the lysozyme molecule is hydrophilic at the ends, while its center is hydrophobic [41]. Hydrophobic interactions will be significant, especially in extreme pH ranges below 3.4 and above 10.0.

3.2. Properties of lysozyme layers on gold surface determined by MP-SPR method, contact angles and infrared spectroscopy

The multi-parameter surface plasmon resonance (MP-SPR) method is widely used for real-time adsorption of many types of biological samples. In the SPR method, the resonance angle depends on the local refractive index of matter located close to the metal surface. For this reason, the method is used when testing the immobilization of particles on metals or functionalized metal surfaces. Lysozyme adsorption was carried out on the gold surface. In the whole range of measurements, lysozyme concentration was 5 ppm, and measurements were carried out in the range of pH 4.0–11.0 at ionic strength $I = 0.01$ M NaCl. Changes in the resonance angle (Θ_{MP-SPR}) during protein adsorption are shown in Fig. 3a, while the mass adsorbed on the sensor surface in Fig. 3b. The adsorbed mass (Γ_{MP-SPR}) increased from 90 ng/cm² at pH = 4.0 to



Schematic 1. Visualization of the charge distribution on the surface of the lysozyme molecule depending on the pH for $I = 0.01$ M NaCl. Designations positive charge - blue, negative - red, neutral - white.

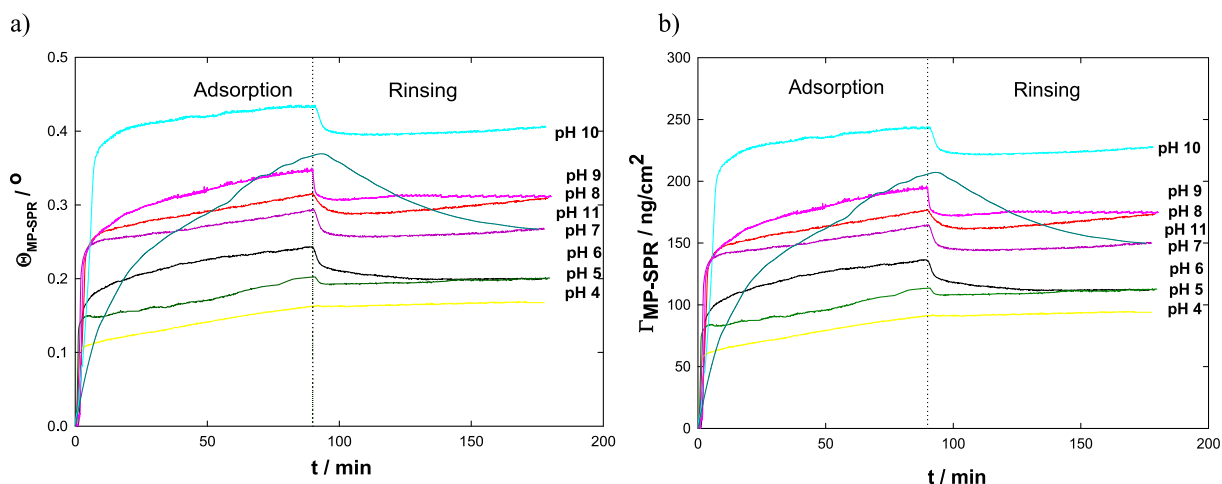


Fig. 3. Adsorption of lysozyme molecules at a concentration of 5 ppm on the Au surface monitored using the MP-SPR method. (a) dependence of the change in the resonance angle (Θ_{MP-SPR}) on time (t) for $I = 0.01$ M, (b) dependence of the change in mass Γ_{MP-SPR} on time (t) for $I = 0.01$ M.

245 ng/cm^2 at $\text{pH} = 10.0$. After exceeding the isoelectric point ($\text{pH} = 10.0$), the adsorbed mass decreased to a level 175 ng/cm^2 for $\text{pH} 11.0$. Higher pH also results in higher desorption, but in the pH range of 4.0–10.0 average desorption is below 5%, which means that lysozyme particles under these conditions are irreversibly adsorbed. Measurements for $\text{pH} = 11.0$ indicate deviations from other measurements for lysozyme. The adsorption curve has a different shape and, moreover, the desorption level is much higher and amounts to 30%. It should be noted that under these conditions both the protein and the surface are negatively charged. In addition, CD studies indicate that in this pH range, there is no significant change in the secondary structure of lysozyme (see Fig. 1).

The adsorbed mass strongly depends on the nature of the interaction between the molecules in the adsorption layer. The orientation of molecules on the surface directly affects the density of the layer. The level of surface coverage depends on the size and shape of adsorbed particles [42,43]. Using the random sequential adsorption (RSA) model for the ellipsoid-shaped molecule [44,45], the weight of adsorbed monolayer for lysozyme (Γ_{RSA}) was determined by the following equation [42]:

$$\Gamma_{RSA} = \frac{M_{LYS}}{S_{LYS}A_v} \theta = \frac{M_{LYS}}{\pi R_H^2 A_v} \theta \quad (2)$$

where M_{LYS} is the molecular weight of lysozyme's molecule ($M_{LYS} = 14.4$ kDa), S_{LYS} is the geometrical cross-sectional area ($S_{LYS} = \pi R_H^2$), A_v - Avogadro's number, while θ is the surface coverage according RSA model for the ellipsoid-shaped molecule.

In the case of asymmetric molecules, the change in the orientation of the molecule in the layer is associated with the change in surface coverage (θ) resulting from the change in the field occupied by the molecule in the adsorption layer. In this case, lysozyme was calculated as the maximum monolayer mass (Γ_{max}), assuming three selected molecular orientations. The obtained results are presented in Table 1.

Based on the MP-SPR results, it was determined that a full monolayer was not formed in the low pH range of 4.0–6.0. Under these conditions, the particles adopt a *side-on* orientation, which means that they strive to achieve the maximum contact area with the oppositely charged gold surface. At $\text{pH} = 7.0$, a full, dense lysozyme monolayer is obtained. Further increase in pH causes reorientation of the molecules on the adsorption surface. The orientation of the molecules induces an increase in adsorbed mass on the sensor surface. However, it cannot be clearly stated whether the molecules assume only *end-on* orientations or whether they occur in *between* or *end-on* orientations (Fig. 4a).

These observations were confirmed by calculating the film thickness based on the MP-SPR and QCM-D results. Up to $\text{pH} = 7$,

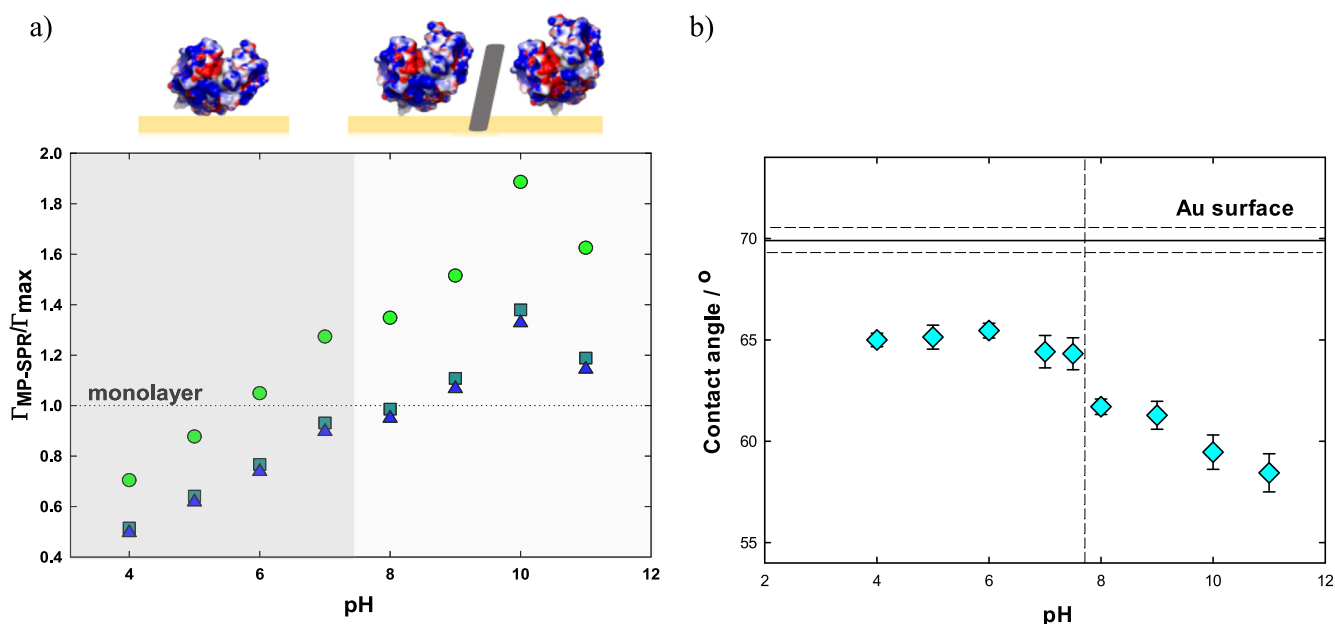
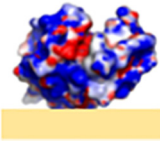
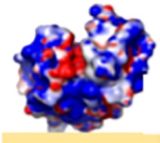
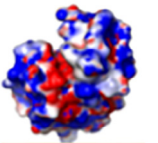


Fig. 4. (a) The ratio of the mass of lysozyme adsorbed on Au surface determined by MP-SPR (Γ_{MP-SPR}) to the maximum mass of the lysozyme monolayer (Γ_{max}) for selected particle orientations: *side-on* (●), *between* (■) and *end-on* (▲), (b) contact angle for lysozyme layers adsorbed on the gold surface at $I = 0.01$ M.

Table 1

Mass of lysozyme monolayer calculated for various molecules' orientation using RSA model. Parameters: S_{LYZ} – geometrical cross-section area for lysozyme, Θ – surface coverage for ellipsoids and close packing model [44], Γ_{max} – maximal mass for monolayer. The dimensions of lysozyme's molecules were taken as $4.5 \times 3.0 \times 3.0$ [25].

Parameters	Orientation		
			
S_{LYZ}/nm^2	10.59	7.47	7.07
Θ	0.577	0.558	0.547
$\Gamma_{max}/ng \times cm^{-2}$	129.38	176.91	183.71

the film thickness is about 3 nm, which corresponds to the shorter size of the lysozyme molecule and *side-on* orientation. In the pH 8–10 range, the layer thickness exceeds 3 nm, which indicates a rearrangement of the molecule to *end-on* orientation or *between* orientation (Table 1S supplementary materials). Confirmation that depending on the orientation of lysozyme molecules forms a monolayer of different thickness are the studies presented by Xu et al. [23].

Measurements carried out by M. Myriam et al. suggest that lysozyme particles on both hydrophobic (methyl) and hydrophilic (silicon oxide) surfaces at pH = 7.4 adsorb in *end-on* orientation [46], but the orientation depends on the degree of surface coverage in the case of low surface coverage protein molecules adopt *side-on* orientations [23]. It should be noted that based on the simulation of molecular dynamics, it was found that at pH = 7.0 the lysozyme molecules assume the orientation *between* on the negatively charged silica surface [41].

The effect of pH on lysozyme adsorption was also assessed by using contact angle measurements (Fig. 4b). For a clean gold surface, a contact angle value of $69.9 \pm 1.2^\circ$ was obtained, which indicates the hydrophobic nature of this surface. Similar results for the gold surface were obtained by Hong et al. 70.2° [47], higher values

of 77.4° were obtained by Parobek and Liu [48]. According to Abdelsalamthe et al. the change in contact angle and surface properties (from hydrophilic to hydrophobic) can be explained by differences in surface topography related to the thickness of the gold layer [49]. Observing how the contact angle of gold changes under the influence of lysozyme adsorption, additional information was obtained about the process of protein adsorption. In the range of pH 4.0–6.0 the contact angle remains stable and is at the level of 65° . A relatively small difference from the initial angle value indicates that the surface coverage of lysozyme is low, and the full monolayer has not been reached. At pH = 7–8.0, contact angles are slightly lower and reach values of 64° and 62° , respectively. At higher pH (9.0–11.5), contact angle values are in the range of 58 – 60° , which means that the surface coverage is saturated, and the surface properties are generated by adsorbed lysozyme particles. The obtained values of contact angles are consistent with the results obtained for the surface of silica and mica modified with lysozyme, where 55° and 57.5° were recorded when full protein monolayers were formed [25,41]. The results of the contact angle correlate with the orientation of the molecule in the adsorption layer, which is associated with the degree of surface coverage. An interesting observation concerns measurement at pH = 11.0,

according to MP-SPR the mass after lysozyme adsorption is at the same level as obtained at pH = 7.0, but the wettability properties of the obtained layers are different.

To determine the effect of adsorption under various pH conditions on the secondary structure of lysozyme, infrared spectroscopy measurements were performed. For this purpose, the polarization-modulation infrared reflection absorption spectroscopy (PM-IRRAS) was used. Qualitatively, the shape of the pH-dependent spectrum of the adsorbed layer looks similar. However, slight changes in the spectrum are visible (Fig. 1S supplement materials), which indicate that the pH at which protein adsorption affects the structure of molecules during adsorption. To perform a quantitative analysis of the structure of the molecule, the spectra were analyzed in the range of amide I (1720–1590 cm⁻¹). The contribution of corresponding secondary structure components has been obtained based on amide I peak deconvolution by using Lorenz-Gaussian fitting, the area under the peaks corresponding to the components of the secondary structure was determined and then their percentage content in the total area of the peak corresponding to amide I was calculated according to the following equation [50]:

$$\text{II - structure component } [\%] = \frac{\text{II - structure component's area}}{\text{area of amide I band}} \quad (3)$$

The location of the component bands of amide I corresponds to the individual fractions of II-structure: 1626 cm⁻¹ band - aggregated β -sheet, 1640 cm⁻¹ - β -sheet, 1659 cm⁻¹ - α -helix, 1666 cm⁻¹ - random coil, while 1684 cm⁻¹ corresponds to β -turn, and 1694 cm⁻¹ - dehydrated β -turn [51]. Changes in spectra of the pH-dependent adsorbed layer are shown in Table 2. The content of β -sheet is represented as the sum of fractions corresponding to the structure of β -sheet and aggregated structures of β -sheet. Contents of turns structures and random were included together. At pH = 3.0 and pH = 6.0, no characteristic band was recorded for the aggregated β -sheet, indicating that these structures are not disturbed. In contrast, at higher pH conditions equal to pH = 11.0 there is an aggregated fraction representing 5% of the total composition, which can mean the start of the aggregation stage of the adsorbed protein.

According to the data presented in Table 2 the adsorption process was followed by a substantial increase in random/ β -turn content, which was accompanied by a significant decrease in the β -sheet fraction and a decrease in α -helix structures, which occurred only at pH = 6.0 and pH = 11.0. At pH = 3.0 the content of α -helix at the same level as in the measurements in solution, indicating that the fraction does not participate in the adsorption of lysozyme on the gold surface. At pH = 6.0 and pH = 11.0, the decrease in α -helix structures is more significant, but for both pH conditions, they occur at a constant level of 19%. This decrease corresponds to the increased random fraction/ β -turn. Similar results of the content for the secondary structure of lysozyme in the adsorbed state were obtained by A. Sethuraman and G. Belfort

[52]. After one-hour adsorption of lysozyme on a hydrophobic self-assembled alkane-thiol(-CN) monolayer the structure of lysozyme at pH = 7.4 consists of α -helix - 23%, β -sheet structures - 12%, and β -turn/random structures - 65%. The extension of lysozyme adsorption time increases the content of β -sheets to 25%, which causes aggregation but without fiber formation. An increase in β -sheets was also observed in the case of lysozyme adsorption on a hydrophilic silica surface [53].

In our case, the fraction with a β -turn/random fraction dominates as a result of the interaction of lysozyme with the gold surface, and the content of β -sheet is low, therefore aggregation does not occur. Earlier studies show that β -turns are necessary for protein folding and stability, they can either provide regions that activate structure formation or passively allow folding to occur, so β -turns can be expected to protect lysozyme in the adsorbed state from aggregation. However, it should be considered that β -turn can prevent the aggregation process by inhibiting interactions that expose regions prone to the association, but too strong interactions can destabilize the local structure, causing frustration leading to incorrect protein folding [54]. The role of β -turn in the structure of the adsorbed protein is still not clearly defined. To elucidate this, further research should be carried out.

A combination of experimental studies with theoretical calculations should enable continued progress in the understanding of the behaviour of proteins on solid surfaces. Development of theoretical methods makes it possible to determine both the interaction of protein molecules with a surface and to visualize the whole process at an atomic level. Basing on MD results can be provide the list of most important residues for protein adsorption at surface, the details of the adsorption process, analysis of the driving forces and the mechanism of protein mobility on the surface, while SMD provides energy barriers for diffusion and desorption [20,4].

3.3. Degree of hydration of lysozyme layers based on QCM-D and MP-SPR results

Lysozyme adsorption on the gold surface was additionally measured using Crystal Microbalance with Dissipation Monitoring (QCM-D) method dedicated to monitoring processes occurring at the solid-liquid interface. During measurements, simultaneously measure two system parameters: changes in the resonant frequency of the sensor (Δf) and energy dissipation (ΔD). Changes in resonance frequency correspond to mass accumulation or mass desorption from the surface of the QCM sensor. The dissipation changes give information on the viscoelastic properties of the layer formed on the sensor. As no considerable differences were noted for successive overtones in the system under examination, all the results were presented for the 7th overtone ($n = 7$).

QCM-D measurements were carried out under identical conditions as in the MP-SPR method. Lysozyme adsorption kinetics obtained using the QCM-D method are shown in Fig. 5a. The increase in sensor frequency corresponds to an increase in adsorbed mass. In the case of lysozyme, the resonance frequency varies from -17 Hz for pH = 4.0 to -27 Hz for pH = 10.0. For pH = 11.0, the slightest drop in resonance frequency was observed. The changes in the value of dissipation per unit of frequency shifts are low and they decrease with increasing pH (Fig. 2S supplement materials). However, in the whole range of selected pH conditions, the energy dissipation did not significantly exceed the value of 1 (Fig. 5b), which indicates that the formed layers are rigid and the Sauerbrey equation is used to estimate the adsorbed mass (Fig. 5c). As the pH increases, an increase in the adsorbed mass on the sensor is observed. Above the isoelectric point of lysozyme, both the gold surface and the protein molecules are negatively charged, resulting in significantly lower adsorption efficiency.

Table 2
The content of II-structure for lysozyme in the adsorbed state in different pH conditions measured by PM-IRRAS and for lysozyme in bulk by CD.

	α -helix/%	β -sheet/%	β -turn/%	Random/%
CD	35.7	31.1	1.2	32.0
PM-IRRAS	35.3	11.4		53.8
pH = 3				
PM-IRRAS	19.2	10.0		70.8
pH = 6				
PM-IRRAS	19.0	15.1		65.9
H = 11				

Under these conditions, desorption reaches the highest level of 29%, while for other conditions, it does not exceed 7%.

The frequency signal rises steeply and linearly with time for $t < 5$ min, after which it slowly starts approaching the saturation value. The occurrence of the linear regime for the initial time indicates that the adsorption of protein is controlled by bulk transport. For longer times of adsorption are visible deviation from the model. In the case of the soft molecules such as proteins observe effect is related with a change orientation of molecules on the surface. Initially protein approach the surface in their native state and bind through some initial contact sites to the surface. Subsequently, structural reorganization take place to this end the conformation changes upon adsorption. This kind of oscillation of adsorption kinetics are reported and explained due to conformational rearrangements [55].

The combination of MP-SPR and QCM-D methods in protein adsorption studies can provide useful information on the degree of hydration of protein layers, which is very useful in biological or biotechnological applications. In Fig. 6a. comparison of results for MP-SPR and QCM-D is presented. It is noteworthy that in the case of QCM-D an increase in the adsorbed mass value is observed from 280 ng/cm^2 for $\text{pH} = 4.0$ to 475 ng/cm^2 for $\text{pH} = 10.0$. The same relationship was observed in the MP-SPR experiments, but the growth factor the mass between the extreme pH values

($\text{pH} = 10.0$ and $\text{pH} = 4.0$) is 1.7 for QCM-D and 2.5 for MP-SPR. In the case of QCM-D, the minimum value of adsorbed mass occurs at $\text{pH} = 11.0$ and is equal to 215 ng/cm^2 , while the adsorbed mass measured by MP-SPR at $\text{pH} = 11.0$ is not minimal, but at a level, as at $\text{pH} = 7.0$. The above observations suggest that different amounts of water bound in the adsorption layer depend on the pH at which the adsorption process was carried out. To calculate the hydration level of lysozyme layers the following equation was used:

$$\Gamma_{H_2O} = \frac{\Gamma_{QCM-D} - \Gamma_{MP-SPR}}{\Gamma_{QCM-D}} \times 100\% \quad (4)$$

where Γ_{MP-SPR} is the adsorbed mass from MP-SPR method, Γ_{QCM-D} is the adsorbed mass from QCM-D method, and Γ_{H_2O} is a fraction of water in the lysozyme film.

The summary of results (Fig. 6b) indicates that the water content of the adsorbed layers of lysozyme is highly dependent on pH. The maximum hydration level of the layer is at the lowest selected pH of 4.0 and decreases with pH, reaching the lowest value at $\text{pH} = 11.0$. According to Fig. 6b the degree of hydration is almost 70% at $\text{pH} = 4.0$, decreases by 5% as the pH scale increases by one to $\text{pH} = 7.0$, and then becomes stable at 50–55% for $\text{pH} = 10.0$. A significant decrease of 20% occurs at $\text{pH} = 11.0$. This trend is well illustrated when the number of water molecules is calculated relative to the number of lysozyme molecules, as shown

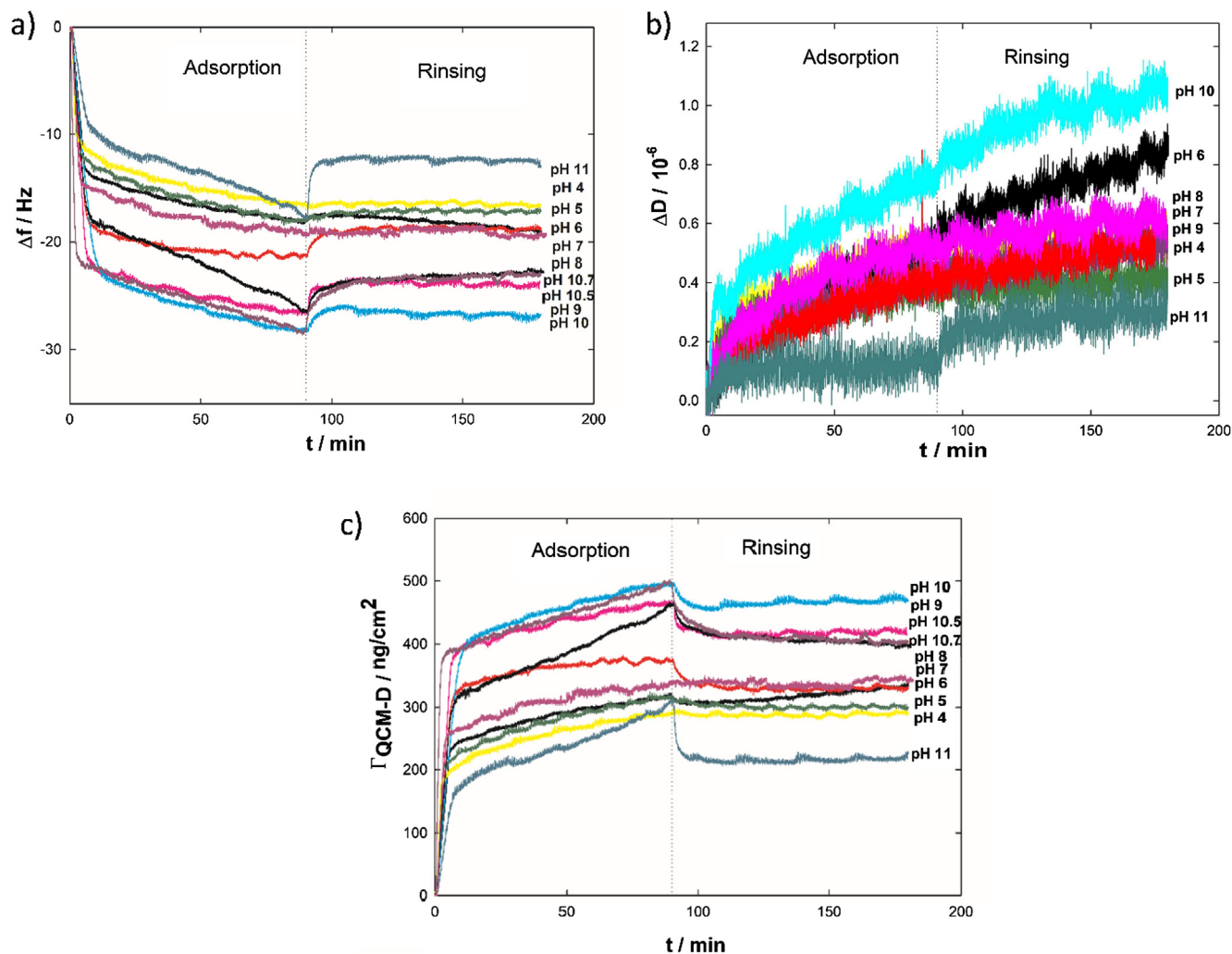


Fig. 5. (a) Dependence of QCM-D sensor resonance frequency changes over time (Δf), (b) dissipation energy (ΔD), (c) adsorbed mass (Γ_{QCM-D}) of lysozyme on the Au sensor for $I = 0.01 \text{ M NaCl}$ depending on pH.

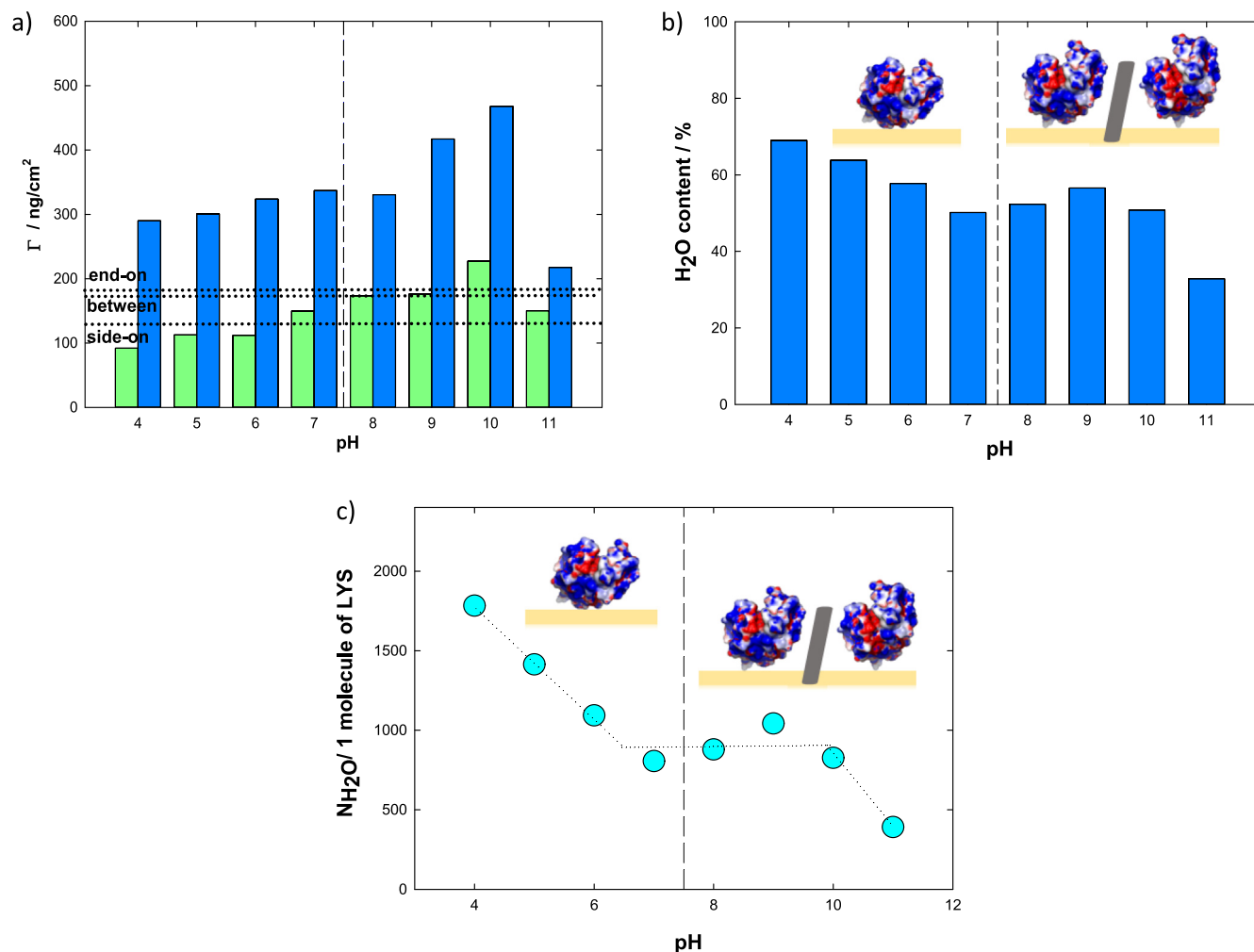


Fig. 6. (a) Comparison of the adsorbed amount of lysozyme mass Γ /ng/cm² on the Au sensor obtained using MP-SPR (green bars) and QCM-D (blue bars) techniques, (b) the percentage of water content in the lysozyme layer on the gold surface, (c) the number of water molecules per one lysozyme molecule in the created layer.

in Fig. 6c. This indicates that in the pH range of 4.0–10.0 hydration is closely related to surface coverage, which in turn is related to the orientation of the molecules in the adsorption layer. In addition, the results obtained are in line with literature data [23] showing that hydration depends on surface coverage and ranges from 50% for a full lysozyme monolayer to 80% with low surface coverage. Similar values for full surface coverage were also obtained by Lundin et al. [56]. However, above the isoelectric point, the trend is not fulfilled, and the water content drops significantly. Considering the results of the zeta potential for the lysozyme molecule, it can be concluded that the higher the positive zeta potential of lysozyme, the greater the mass of water associated with the protein layer, which indicates that the hydration of lysozyme increases with its uncompensated positive charge.

4. Conclusions

In the presented work, we selected hen egg lysozyme and gold surface to study factors having a major impact on the mechanism of protein adsorption and the hydration of the protein layer on the solid surface. By using surface plasmon resonance the nature of the interactions and related amount of adsorbed protein were investigated and allowed us to determine an orientation of molecules on the gold surface. Experimental data were compared with the

Random Sequential Adsorption model for a molecule with an ellipsoidal shape. In the range of low surface coatings, the protein is adsorbed in a *side-on* orientation, with an increase in surface coverage above $\Gamma = 130$ ng/cm² the protein is reoriented. Lysozyme's tendencies to change orientation are confirmed by literature data [17,46]. The rearrangement of molecules in the adsorption layer is manifested in the macroscopic properties of the layers formed. As a consequence, higher surface coverage is associated with an increase in the degree of hydrophilicity of the formed layer.

Lysozyme is considered a stable protein, as confirmed by the obtained CD spectra. PM-IRRAS measurements respectively showed changes in the secondary structure of lysozyme as a result of the interaction between the protein and the gold surface. There is a significant increase in β -turn/random content, while the β -sheet fraction decreases. These changes do not induce protein aggregation, although the β -turn is responsible for stabilizing the secondary structure. The high stability of α -helix structures at pH = 3.0 means that under these conditions, they do not directly participate in surface interactions. At higher pH (spectra for pH = 6.0 and pH = 11.0) changes in this range can be seen. Aggregation tendencies are also observed in such conditions. It should be noted here that the native pH for lysozyme is a pH range of 4.0–5.0 and under these conditions, it adopts an optimal structure.

Parallel measurements using MP-SPR and QCM-D allow estimating not only the efficiency of protein adsorption but also the

change in hydration of the layers formed on the gold surface. Along with the change in pH, a change in adsorption efficiency is observed but also a change in the degree of hydration. At pH = 4.0 the degree of hydration is at the level of 70% but with a change in pH, it decreases to 30%. The obtained results indicate that hydration of the layer is mainly related to the degree of protonation of the protein molecule.

The presented data indicate that the surface coating is directly correlated with the charge of protein particles and has a significant impact on the properties of the protein film deposited on the surface of gold, which is especially crucial from designing new materials for biological applications.

Declaration of Competing Interest

The authors declare that they have no known competing financial interests or personal relationships that could have appeared to influence the work reported in this paper.

Acknowledgments

The presented work was partially supported by Grant NCN OPUS 2016/23/B/ST5/02788, Grant NAWA PPN/BIL/2018/1/00103, and Grant POWR03.02.0000-1013/16. The authors would also like to acknowledge Izabella Brand for support in PM-IRRAS spectra analysis and Maciej Tworek for help in preparing graphical abstract.

Appendix A. Supplementary material

Supplementary data to this article can be found online at <https://doi.org/10.1016/j.bioelechem.2020.107582>.

References

- [1] S. Barr, E.W. Hill, A. Bayat, Novel proteomic assay of breast implants reveals proteins with significant binding differences: implications for surface coating and biocompatibility, *Aesthetic Surg. J.* 38 (2018) 962–969, <https://doi.org/10.1093/asj/sjy018>.
- [2] F. Romero-Gavilana, N. Araújo-Gomes, A.M. Sánchez-Pérez, I. García-Arnáez, F. Elortza, M. Azkargorta, J.J. Martín de Llano, C. Carda, M. Gurruchaga, J. Suay, I. Goñi, Bioactive potential of silica coatings and its effect on the adhesion of proteins to titanium implants, *Colloids Surf. B: Biointerfaces* 162 (2018) 316–325, <https://doi.org/10.1016/j.colsurfb.2017.11.072>.
- [3] J.N. Walker, C.L. Pinkner, A.J.L. Lynch, S. Orbal, J.S. Pinkner, S.J. Hultgren, T.M. Myckatyn, Deposition of host matrix proteins on breast implant surfaces facilitates staphylococcus epidermidis biofilm formation: in vitro analysis, *Aesthetic Surg. J.* (2019) sjz099, <https://doi.org/10.1093/asj/sjz099>.
- [4] M. Martínez-Hernández, V.I. García-Pérez, A. Almaguer-Flores, Potential of salivary proteins to reduce oral bacterial colonization on titanium implant surfaces, *Mater. Lett.* 252 (2019) 120–122, <https://doi.org/10.1016/j.matlet.2019.05.089>.
- [5] Y. Loo, M. Goktas, A.B. Tekinay, M.O. Guler, C.A.E. Hauser, A. Mitrak, Self-assembled proteins and peptides as scaffolds for tissue regeneration, *Adv. Healthcare Mater.* 18 (2015) 2557–2586, <https://doi.org/10.1002/adhm.201500402>.
- [6] L. Wan-Geun, P. Saibom, Y. Hee-Hun, J. Gun-Jae, L. Tae-Jin, B. Suk Ho, H. Jeong Yeon, C. Kookheon, K. Byung-Soo, Delivery of a therapeutic protein for bone regeneration from a substrate coated with graphene oxide, *Small: nano micro* 9 (23) (2013) 4051–4060, <https://doi.org/10.1002/sml.201300571>.
- [7] Z. Wang, Y. Zhang, J. Zhang, L. Huang, J. Liu, Y. Li, G. Zhang, S.C. Kundu, L. Wang, Exploring natural silk protein sericin for regenerative medicine: an injectable, photoluminescent, cell-adhesive 3D hydrogel, *Sci. Rep.* 4 (7064) (2014) 1–11, <https://doi.org/10.1038/srep07064>.
- [8] Y. Krishnan, H.A. Rees, C.P. Rossitto, S.E. Kim, H.H.K. Hun, G.E.H. Frank, B.D. Olsen, D.R. Liu, P.T. Hammond, A.J. Grodzinsky, Green fluorescent proteins engineered for cartilage-targeted drug delivery: Insights for transport into highly charged avascular tissues, *Biomaterials* 183 (2018) 218–233, <https://doi.org/10.1016/j.biomaterials.2018.08.050>.
- [9] Q. Peng, H. Mu, The potential of protein–nanomaterial interaction for advanced drug delivery, *J. Control. Release* 225 (2016) 121–132, <https://doi.org/10.1016/j.jconrel.2016.01.041>.
- [10] D. Sleep, Albumin and its application in drug delivery, *Expert Opin. Drug Deliv.* 12 (5) (2014) 793–812, <https://doi.org/10.1517/17425247.2015.993313>.
- [11] K. Tokarczyk, B. Jachimska, Characterization of G4 PAMAM dendrimer complexes with 5-fluorouracil and their interactions with bovine serum albumin, *Colloids Surf., A* 561 (2018) 357–363, <https://doi.org/10.1016/j.colsurfa.2018.10.080>.
- [12] S. Świątek, P. Komorek, G. Turner, B. Jachimska, β -Lactoglobulin as a potential carrier for bioactive molecules, *Bioelectrochemistry* 126 (2019) 137–145, <https://doi.org/10.1016/j.bioelechem.2018.12.006>.
- [13] M. Kulkarni, A. Mazare, J. Park, E. Gongadze, M.S. Killian, S. Kralj, K. Mark, A.P. Schmuki, Protein interactions with layers of TiO₂ nanotube and nanopore arrays: morphology and surface charge influence, *Acta Biomaterialia* 45 (2016) 357–366, <https://doi.org/10.1016/j.actbio.2016.08.050>.
- [14] D. Doctor, S. Strieth, D. Westmeier, O. Hayden, M. Gao, S.K. Knauer, R.H. Stauber, No king without a crown – impact of the nanomaterial–protein corona on nanobiomedicine, *Nanomedicine* 10 (3) (2015) 503–519, <https://doi.org/10.2217/nnm.14.184>.
- [15] S.A. Bhakta, E. Evans, T.E. Benavidez, C.D. Garcia, Protein adsorption onto nanomaterials for the development of biosensors and analytical devices: a review, *Anal. Chem. Acta* 872 (2015) 7–25, <https://doi.org/10.1016/j.aca.2014.10.031>.
- [16] A.A. Feiler, A. Sahlholm, T. Sandberg, K.D. Caldwell, Adsorption and viscoelastic properties of fractionated mucin (BSM) and bovine serum albumin (BSA) studied with quartz crystal microbalance (QCM-D), *J. Colloid Interface Sci.* 315 (2) (2007) 475–481, <https://doi.org/10.1016/j.jcis.2007.07.029>.
- [17] C.G. Marxer, M.C. Coen, L. Schlappbach, Study of adsorption and viscoelastic properties of proteins with a quartz crystal microbalance by measuring the oscillation amplitude, *J. Colloid Interface Sci.* 261 (2) (2003) 291–298, [https://doi.org/10.1016/S0021-9797\(03\)00089-4](https://doi.org/10.1016/S0021-9797(03)00089-4).
- [18] A.W. Sonesson, T.H. Callisen, H. Brismar, U.M.A. Elofsson, A comparison between dual polarization interferometry (DPI) and surface plasmon resonance (SPR) for protein adsorption studies, *Colloids Surf. B: Biointerfaces* 54 (2) (2007) 236–240, <https://doi.org/10.1016/j.colsurfb.2006.10.028>.
- [19] T. Becherer, C. Grunewald, V. Engelschalt, G. Multhaupt, T. Risse, R. Haag, Polyglycerol based coatings to reduce non-specific protein adsorption in sample vials and on SPR sensors, *Anal. Chim. Acta* 867 (2015) 47–55, <https://doi.org/10.1016/j.aca.2015.01.048>.
- [20] K. Kubiak-Ossowska, K. Tokarczyk, B. Jachimska, P.A. Mulheran, Bovine serum albumin adsorption at a silica surface explored by simulation and experiment, *J. Phys. Chem. B* 121 (16) (2017) 3975–3986, <https://doi.org/10.1021/acs.jpcc.7b01637>.
- [21] B. Kalas, J. Nador, E. Agocs, A. Saftics, S. Kuruncz, M. Fried, P. Petrik, Protein adsorption monitored by plasmon-enhanced semi-cylindrical Kretschmann ellipsometry, *Appl. Surf. Sci.* 421 (2017) 585–592, <https://doi.org/10.1016/j.apsusc.2017.04.064>.
- [22] G. Guzman, S.M. Bhaway, T. Nugay, B.D. Vogt, M. Cakmak, Transport-limited adsorption of plasma proteins on bimodal amphiphilic polymer co-networks: real-time studies by spectroscopic ellipsometry, *Langmuir* 33 (11) (2017) 2900–2910, <https://doi.org/10.1021/acs.langmuir.7b00281>.
- [23] K. Xu, M.M. Oubera, M.E. Welland, A comprehensive study of lysozyme adsorption using dual polarization interferometry and quartz crystal microbalance with dissipation, *Biomaterials* 34 (2013) 1461–1470, <https://doi.org/10.1016/j.biomaterials.2012.10.078>.
- [24] X. Wu, G. Narsimhan, Effect of surface concentration on secondary and tertiary conformational changes of lysozyme adsorbed on silica nanoparticles, *Biochim. Biophys. Acta (BBA) - Proteins Proteomics* 1784 (11) (2008) 1694–1701, <https://doi.org/10.1016/j.bbapap.2008.06.008>.
- [25] B. Jachimska, A. Kozłowska, A. Pajor-Świerzy, Protonation of lysozymes and its consequences for the adsorption onto a mica surface, *Langmuir* 28 (31) (2012) 11502–11510, <https://doi.org/10.1021/la301558u>.
- [26] B. Jachimska, A. Pajor, Physico-chemical characterization of bovine serum albumin in solution and as deposited on surfaces, *Bioelectrochemistry* 87 (2012) 138–146, <https://doi.org/10.1016/j.bioelechem.2011.09.004>.
- [27] M. Sumarokova, J. Iturri, A. Weber, M. Maeres, C. Keil, H. Haase, J.L. Toca-Herrera, Influencing the adhesion properties and wettability of mucin protein films by variation of the environmental pH, *Sci. Rep.* 8 (2018) 9660, <https://doi.org/10.1038/s41598-018-28047-z>.
- [28] P. Bingen, G. Wang, N.F. Steinmetz, M. Rodahl, R.P. Richter, Solvation effects in the quartz crystal microbalance with dissipation monitoring response to biomolecular adsorption. A phenomenological approach, *Anal. Chem.* 80 (23) (2008) 8880–8890.
- [29] R.N. Rambaran, L.C. Serpell, Amyloid fibrils. Abnormal protein assembly, *Prion* 2 (3) (2008) 112–117, <https://doi.org/10.4161/pri.2.3.7488>.
- [30] S.S. Wang, Y.T. Hung, P. Wang, J.W. Wu, The formation of amyloid fibril-like hen egg-white lysozyme species induced by temperature and urea concentration-dependent denaturation, *Biotechnology* 24 (2007) 787–795, <https://doi.org/10.1007/s11814-007-0042-6>.
- [31] S. Kumar, V.K. Ravi, R. Swaminathan, Suppression of lysozyme aggregation at alkaline pH by tri-N-acetylchitotriose, *Biochim. Biophys. Acta (BBA) - Proteins Proteomics* 1794 (6) (2009) 913–920, <https://doi.org/10.1016/j.bbapap.2009.01.009>.
- [32] J. Wawer, M. Szociński, M. Olszewski, R. Piątek, M. Naczek, J. Krakowiak, Influence of the ionic strength on the amyloid fibrillogenesis of hen egg white lysozyme, *Int. J. Biol. Macromol.* 121 (2019) 63–70, <https://doi.org/10.1016/j.ijbiomac.2018.09.165>.
- [33] B. Moores, E. Drolle, S.J. Attwood, J. Simons, Z. Leonenko, Effect of surfaces on amyloid fibril formation, *PLoS One* 6 (10) (2011), <https://doi.org/10.1371/journal.pone.0025954> e25954.

- [34] B. Russell, B. Jachimska, P. Komorek, P. Mulheran, Y. Chen, Lysozyme encapsulated gold nanoclusters: effects of cluster synthesis on natural protein characteristics, *Phys. Chem. Chem. Phys.* 19 (10) (2017) 7228–7235, <https://doi.org/10.1039/C7CP00540G>.
- [35] G. Holzwarth, P. Doty, The ultraviolet circular dichroism of polypeptides, *J. Am. Chem. Soc.* 87 (1965) 218–228, <https://doi.org/10.1021/ja01080a015>.
- [36] N. Greenfield, G.D. Fasman, Computed circular dichroism spectra for the evaluation of protein conformation, *Biochemistry* 8 (1969) 4108–4116, <https://doi.org/10.1021/bi00838a031>.
- [37] S.W. Provencher, J. Glockner, Estimation of globular protein secondary structure from circular dichroism, *Bioelectrochemistry* 20 (1) (1981) 30–37, <https://doi.org/10.1021/bi00504a006>.
- [38] B. Jachimska, S. Świątek, J.I. Loch, K. Lewiński, T. Luxbacher, Adsorption effectiveness of β -lactoglobulin onto gold surface determined by quartz crystal microbalance, *Bioelectrochemistry* 121 (2018) 95–104, <https://doi.org/10.1016/j.bioelechem.2018.01.010>.
- [39] L.R. Wetter, H.F. Deutsh, Immunological studies of egg white proteins. Immunological and physical studies of lysozyme, *J. Biol. Chem.* 192 (1) (1951) 237–242.
- [40] C.A. Haynes, W. Norde, Globular proteins at solid/liquid interfaces, *Colloids Surf. B: Biointerfaces* 2 (6) (1994) 517–566, [https://doi.org/10.1016/0927-7765\(94\)80066-9](https://doi.org/10.1016/0927-7765(94)80066-9).
- [41] K. Kubiak, M. Cwieka, M.A. Kaczynska, B. Jachimska, P.A. Mulheran, Lysozyme adsorption at a silica surface using simulation and experiment: effects of pH on protein layer structure, *Phys. Chem. Chem. Phys.* 17 (2015) 24070–24077, <https://doi.org/10.1039/C5CP03910J>.
- [42] R. Pericet-Camara, G. Papastavrou, M. Borkovec, Effective charge of adsorbed poly(amido amine) dendrimers from direct force measurements, *Macromolecules* 42 (2009) 1749–1758, <https://doi.org/10.1021/ma802374z>.
- [43] Z. Adamczyk, *Particles at Interfaces; Interaction, Deposition, Structure*, Publisher: Interface Sciences and Technology, London, The United Kingdom, 2006, pp. 1–743.
- [44] J.D. Sherwood, Random sequential adsorption of lines and ellipses, *J. Phys. A: Math. Gen.* 23 (13) (1990) 2827–2833, <https://doi.org/10.1119/1.5049954>.
- [45] M. Cieřla, G. Pająk, R. Ziff M., In a search for a shape maximizing packing fraction for two-dimensional random sequential adsorption, *J. Chem. Phys.* 145 (4) (2016), <https://doi.org/10.1063/1.4959584> 044708.
- [46] M.M. Ouberaï, K. Xu, M.E. Welland, Effect of the interplay between protein and surface on the properties of adsorbed protein layers, *Biomaterials* 35 (2014) 6157–6163, <https://doi.org/10.1016/j.biomaterials.2014.04.012>.
- [47] D. Hong, K. Bae, S.P. Hong, J.H. Park, I.S. Choi, W.K. Cho, Mussel-inspired, perfluorinated polydopamine for self-cleaning coating on various substrates, *Chem. Commun.* 50 (2014) 11649–11652, <https://doi.org/10.1039/C4CC02775B>.
- [48] D. Parobek, H. Liu, Wettability of graphene, *2D Materials* 2 (3) (2015) 032001, <https://doi.org/10.1039/C8NH00348C>.
- [49] M.E. Abdelsalam, P.N. Bartlett, T. Kelf, J. Baumberg, Wetting of regularly structured gold surfaces, *Langmuir* 21 (51) (2005) 1753–1757, <https://doi.org/10.1021/la047468q>.
- [50] A. Barth, Infrared spectroscopy of proteins, *Biochim. Biophys. Acta (BBA) – Bioenergetics* 1767 (9) (2007) 1073–1101, <https://doi.org/10.1016/j.bbabi.2007.06.004>.
- [51] C.L. Wilder, A.D. Friedrich, R.O. Potts, G.O. Daumy, M.L. Francoeur, Secondary structural analysis of two recombinant murine proteins, interleukins 1 alpha and 1 beta: is infrared spectroscopy sufficient to assign structure, *Biochemistry* 31 (1) (1992) 27–31, <https://doi.org/10.1021/bi00116a006>.
- [52] A. Sethuraman, G. Belfort, Protein structural perturbation and aggregation on homogeneous surfaces, *Biophys. J.* 88 (2005) 1322–1333, <https://doi.org/10.1529/biophysj.104.051797>.
- [53] S.M. Daly, T.M. Przybycien, R.T. Tilton, Aggregation of lysozyme and of poly(ethylene glycol)-modified lysozyme after adsorption to silica, *Colloids Surf. B: Biointerfaces* 57 (2007) 81–88, <https://doi.org/10.1016/j.colsurfb.2007.01.007>.
- [54] A.M.C. Marcelino, L.M. Gierasch, Roles of β -turns in protein folding: from peptide models to protein engineering, *Biopolymers* 89 (5) (2008) 380–391, <https://doi.org/10.1002/bip.20960>.
- [55] M. Rabe, D. Verdes, S. Seeger, Understanding protein adsorption phenomena at solid surfaces, *Adv. Colloid Interface Sci.* 162 (2011) 87–106, <https://doi.org/10.1016/j.cis.2010.12.007>.
- [56] M. Lundin, U.M. Elofsson, E. Blomberg, M.W. Rutland, Adsorption of lysozyme, β -casein and their layer-by-layer formation on hydrophilic surfaces: effect of ionic strength, *Colloids Surf. B: Biointerfaces* 77 (2010) 1–11, <https://doi.org/10.1016/j.colsurfb.2009.12.019>.